Physicochem. Probl. Miner. Process., 62(4), 2026, 231151

http://www.journalssystem.com/ppmp

Physicochemical Problems of Mineral Processing

ISSN 1643-1049

Selective recovery of cobalt and nickel from spent lithium-ion batteries by integrated roasting and chelation-assisted deep eutectic solvent leaching

Eon-Seok Sim, Seok-Young Oh

Department of Civil and Environmental Engineering, University of Ulsan, Ulsan 44610, South Korea

Corresponding author: quartzoh@ulsan.ac.kr (Seok-Young Oh)

Abstract: The growing adoption of electric vehicles is expected to result in a significant increase in the volume of spent lithium-ion batteries (LIBs), highlighting the need for efficient and environmentally sustainable recycling methods. This study presents an optimized process for recovering critical metals—cobalt, nickel, manganese, and lithium—from spent LIBs. The method involves roasting followed by leaching using a deep eutectic solvent (DES) composed of propionic acid (PA), choline chloride (ChCl), and nitrilotriacetic acid (NTA), a chelating agent. Key operational parameters—including roasting temperature and duration, ChCl–PA molar ratio, leaching temperature and time, solid-to-liquid ratio, and NTA concentration—were systematically investigated. Roasting at 200 °C for 2 h improved leaching efficiencies of nickel and cobalt by 20.2% and 6.3%, respectively. Optimal leaching conditions were identified as 80 °C for 120 min with a solid-to-liquid ratio of 15 g/L. The addition of 0.07 M NTA shortened the leaching time from 120 to 60 min while achieving leaching efficiencies of 98.5% for lithium and 100% for cobalt, nickel, and manganese. Manganese was selectively separated from the leachate using D2EHPA, while cobalt, nickel, and lithium were subsequently recovered from the manganese-free solution using Cyphos IL 104 and oxalic acid. Leaching efficiency declined by 10–15% with each reuse of the DES. Overall, this approach offers a highly efficient and economically feasible strategy for metal recovery from spent LIBs, contributing to circular economy practices and sustainable battery waste management.

Keywords: deep eutectic solvent, spent lithium-ion batteries, metal recovery, eco-friendly leaching, reductive roasting

1. Introduction

Since the pioneering work of researchers in the late 1970s and early 1980s utilizing cobalt oxides and lithium metals (Whittingham et al., 1976; Mizushima et al., 1980), lithium-ion batteries (LIBs) have undergone rapid technological advancement. These developments have positioned LIBs as the leading energy storage system for portable electronics and electric vehicles (EVs). The commercialization of EVs accelerated in the 2010s, with increasing emphasis on high-performance batteries and environmentally sustainable practices aimed at reducing carbon emissions. As a result, EVs have emerged as a viable global alternative to conventional transportation (Liu et al., 2023). According to the International Energy Agency (2024), the continued growth in EV adoption will lead to a significant increase in end-of-life LIBs. In South Korea alone, 440 EV battery packs were discarded in 2021, with projections reaching approximately 80,000 by 2029—corresponding to a resource value of nearly 200 billion KRW (KISTI Data Analysis Department, 2021).

This rising volume of battery waste presents serious environmental and resource management challenges. Improper disposal of spent batteries poses environmental risks, including soil and groundwater contamination from leached heavy metals and toxic compounds (Peters et al., 2017; Mrozik et al., 2021). Moreover, global shortages of critical metals such as nickel (Ni), cobalt (Co), and lithium (Li) threaten economic and industrial stability. As of 2023, Co and Ni prices stand at approximately $33,000 and $15,000 per metric ton, respectively (Trading Economics, 2023). Price

DOI: 10.37190/ppmp/231151

volatility not only increases battery production costs but also underscores the importance of recovering these metals through recycling. Supply chain instability further exacerbates risks to the battery industry, potentially causing disruptions, production delays, and increased costs (Egbue and Long, 2012; Olivetti et al., 2017; BGS, 2018). Efficient recycling of end-of-life LIBs is therefore essential for both environmental protection and strategic resource recovery.

Conventional battery recycling techniques include pyrometallurgical, hydrometallurgical, and direct recycling methods, each with distinct advantages and limitations. Pyrometallurgy involves smelting to recover valuable metals but is associated with high energy consumption, Li loss to slag, and low overall resource recovery efficiency (Makuza et al., 2021; Liu et al., 2019). In addition, high operating costs constrain its economic feasibility (Reinhart et al., 2023). Direct recycling, which focuses on regenerating electrode materials, significantly reduces energy use and greenhouse gas emissions. For instance, lithium iron phosphate (LFP) cells can be regenerated for $2.1 per kilogram (Xu et al., 2020). However, the manual disassembly required to separate the anode and cathode components limits scalability. Diverse pouch cell formats also complicate automation (Ji et al., 2021). Hydrometallurgy, the most widely used commercial method, employs inorganic acids (e.g., sulfuric or hydrochloric acid) and reducing agents (e.g., hydrogen peroxide) to extract metals. While it offers high metal recovery and selectivity (Dalini et al., 2020), it generates corrosive waste and harmful emissions (Cl_2, SO_x, NO_x), posing environmental concerns (Meshram et al., 2020). Although organic acids have been proposed as alternatives, challenges such as high cost, slow kinetics, and limited scalability hinder their industrial application (Li et al., 2013; Yao et al., 2018).

One of the major drawbacks of the hydrometallurgical process is that a large dosage of chemicals may be needed to leach the valuable metals from cathode materials in the spent LIBs. To overcome this barrier, environment-friendly deep eutectic solvents (DESs) have been intensively applied to extract the metals from the spent LIBs, and the reuse of spent DESs has also been studied (Wang et al., 2022; Qiao et al., 2024). DESs have gained attention as environmentally benign alternatives that enable efficient metal recovery with minimal secondary pollution. DESs consist of hydrogen bond acceptors (HBAs) and donors (HBDs) that interact through hydrogen bonding to form a liquid phase at reduced melting points (Smith et al., 2014; Kudlak et al., 2015). Their tunable physical properties facilitate the dissolution of polar species, including metal ions. DESs are typically non-volatile, reusable, and less toxic than conventional solvents, leading to reduced waste generation (Radosevic et al., 2015; 2016; Padwal et al., 2022; Wang et al., 2022; Qiao et al., 2024). Initial studies demonstrated the high efficiency of DESs in metal recovery from LIBs. For instance, a choline chloride–ethylene glycol DES recovered 99.3% of Li and Co from lithium cobalt oxide (LCO) batteries (Tran et al., 2019). Other combinations, such as choline chloride–ethylene glycol and choline chloride–formic acid, showed recovery rates exceeding 90% for multiple metals under high-temperature and prolonged leaching conditions (Chen et al., 2021; Schiavi et al., 2021). A DES composed of dimethyl-beta-propiothetin and ethylene glycol achieved recovery efficiencies of 99.6% (Li), 99.3% (Ni), 99.0% (Co), and 99.5% (Mn) within 60 min at 100 °C (Luo et al., 2024). Similarly, a DES of betaine hydrochloride and ethylene glycol achieved recovery rates of 91.0% (Li), 93.1% (Ni), 93.0% (Co), and 82.4% (Mn) in just 20 min at 140 °C (Luo et al., 2023). Although these findings demonstrate the potential of DESs, challenges such as long leaching times and the need for elevated temperatures persist.

Anaerobic roasting of spent LIB cell powder is a carbothermal reduction process conducted under an oxygen-free atmosphere, in which the graphite inherently present in the cell powder acts as an in-situ reducing agent (Pan and Shen, 2023; Shen and Zhang, 2025; Zadeh et al., 2026). During heating, the decomposition of residual electrolyte and polymeric binders generates reducing gases, while the layered structure of $LiNi_xCo_yMn_zO_2$ (NCM) gradually collapses because lithium is released from the crystal lattice. Simultaneously, graphite reacts with lattice oxygen to produce CO, which further promotes the reduction of transition-metal oxides under reducing conditions (Pan and Shen, 2023). As a result, Ni and Co oxides are readily reduced to metallic phases, whereas Mn is generally reduced only to MnO due to its higher thermodynamic stability. Meanwhile, lithium is converted into Li_2CO_3 through reaction with CO_2 generated during carbothermal reduction, enabling its selective recovery by subsequent water leaching. These phase transformations significantly destabilize the original cathode structure and increase the chemical reactivity of the roasted products. Consequently, anaerobic roasting

changes the chemical phases of transition metals, resulting in enhanced leaching kinetics, reduced acid consumption, and improved metal recovery efficiency during downstream hydrometallurgical processing. Therefore, anaerobic roasting has recently attracted considerable attention as an effective pretreatment technology for the recycling of spent LIBs (Shen and Zhang, 2025).

To overcome the limitation in application DES alone, the present study introduces a novel approach that combines reductive roasting and the use of chelating agents to enhance the solubility of metal ions and accelerate leaching kinetics. The integration of DES with reductive roasting and chelating agents enables a more efficient, lower-temperature process for metal recovery (Fig. S1). Through a series of batch experiments, the effects of key operational parameters on leaching performance were investigated, and optimal conditions were determined. Leaching efficiencies for Co, Ni, Mn, and Li were evaluated under these conditions. In addition, a sequential solvent extraction process was developed to selectively separate and precipitate individual metals as precursors for battery material synthesis. The reusability of the DES system was also assessed to evaluate its environmental and economic viability.

2. Materials and methods

2.1. Materials

Propionic acid (PA, $C_3H_6O_2$, 99.5%), choline chloride (ChCl, $C_5H_{14}ClNO$, 98%), nitrilotriacetic acid (NTA, $C_6H_9NO_6$, 99%), di(2-ethylhexyl)phosphoric acid (D2EHPA, $C_{16}H_{35}O_4P$, 97%), Cyphos IL 104 ($C_{48}H_{102}O_2P_2$, 90%), kerosene (99%), oxalic acid ($C_2H_2O_4$, 98%), sulfuric acid (H_2SO_4, 95%), sodium hydroxide (NaOH, 98%), $NiCl_2 \cdot 6H_2O$ (99.9%), and $CoCl_2 \cdot 6H_2O$ (99.9%) were purchased from Aldrich (Milwaukee, WI, USA). Deionized water (DIW) was produced using a Nex Power 1000 system (Human, Seoul, South Korea). Cell powder from spent LIBs was supplied by Sungeel Hitech (Gunsan, Jeonbuk, South Korea), where the batteries were pretreated via discharge, disassembly, thermal processing, and crushing. All chemicals were of analytical grade and used without further purification.

2.2. Methods

2.2.1. Roasting of cell powder

Roasting was performed using an activation reactor (J-AC1000, Jisico, Seoul, South Korea) equipped with a high-temperature furnace capable of stable operation up to 1100 °C. Approximately 10 g of pretreated cell powder was placed in a crucible and heated to 200 °C at a rate of 10 °C/min under a nitrogen flow of 200 mL/min, then maintained at that temperature for 2 h. The effects of roasting temperature (100–800 °C) and time (30–150 min) were systematically investigated.

2.2.2. Leaching of cell powder with DES

The DES was prepared by mixing ChCl (hydrogen bond acceptor, HBA) and PA (hydrogen bond donor, HBD) in a 1:1.5 molar ratio, with the addition of 30 wt.% DIW to enhance metal extraction. Preliminary tests confirmed this molar ratio as optimal for metal ion dissolution. Leaching experiments were conducted in 250 mL amber glass vials using 0.5–2.5 g of cell powder and 100 mL of DES under varying conditions: temperature (20–140 °C), leaching time (20–140 min), and solid-to-liquid ratios (5–25 g/L). The DES–cell powder mixtures were stirred using a temperature-controlled magnetic stirrer. After leaching, a 1 mL aliquot was filtered through a 0.45 µm cellulose membrane (Hyundai Micro, Gyeonggi, South Korea) to separate solids from the leachate. Concentrations of Co and Ni were analyzed. To improve leaching efficiency and reduce reaction time, NTA was added as a chelating agent. Direct addition of both NTA and cell powder caused foaming and overflow; thus, NTA was pre-dissolved in the DES before introducing the powder. NTA concentrations were varied in 0.03 M increments up to 0.1 M under optimized conditions. At the optimal NTA concentration, leaching time was gradually reduced from 120 to 50 min (10-min intervals), and metal recovery was evaluated. All experiments were conducted in triplicate to ensure accuracy and precision. Metal leaching efficiency (η_i, %) was calculated using Eq. 1 (Yan et al., 2023):

$$\eta_i = 100 \times \frac{c_i V}{m_0 w_i} \quad (1)$$

where m_0 is the mass of the raw material, g; w_i is the mass percentage of element i in the raw material. C_i is the concentration of element i in the leachate, g/mL; and V is the volume of leachate, mL.

2.2.3. Solvent extraction of metals from leachate

Mn, Co, Ni, and Li were selectively recovered from the leachate using organic solvents. Initially, Mn was extracted from the aqueous phase using 0.6 M D2EHPA diluted in kerosene as the organic phase. The pH of the aqueous phase was adjusted to 2.5 using 1 M sulfuric acid and 1 M sodium hydroxide, and the organic-to-aqueous phase volume ratio was maintained at 1:1. To enhance the extraction kinetics, the mixture was vigorously stirred at 40 °C for 20 min. Subsequently, the phases were separated by centrifugation at 3000 rpm, and Mn was recovered by stripping the organic phase with 1 M sulfuric acid (Nadimi and Jalalian Karazmoudeh, 2021; Vieceli et al., 2023). Cobalt extraction was performed using 20 vol.% Cyphos IL 104. Following a similar procedure to that used for Mn extraction, the aqueous phase pH was adjusted to 4.5, and the extraction was conducted under identical conditions, except for the solvent. Co was then stripped using 1 M sulfuric acid, and cobalt hydroxide was precipitated by raising the pH above 7 (Rybka and Regel-Rosocka, 2012; Wellens et al., 2013; Mishra et al., 2020; Yuda et al., 2024). After Mn and Co removal, Ni was recovered by precipitation as nickel oxalate through the addition of 1 M oxalic acid (Yao et al., 2018; Li et al., 2021). Lithium remained in the aqueous phase, which was subjected to evaporation by adding ethanol and heating at 80 °C for 12 h to recover Li as lithium oxalate (Hua et al., 2022). The remaining DES was recovered and reused for leaching the cell powder to evaluate its reusability under the optimal conditions established in this study.

2.2.4. Analytical methods

The metal contents in the cell powder were determined using X-ray fluorescence spectroscopy (XRF; SEA1200VX, SII Nano Technology Inc., Tokyo, Japan) and inductively coupled plasma optical emission spectroscopy (ICP-OES; 700-ES, Varian, Palo Alto, CA, USA). Ultraviolet-visible (UV-vis) spectroscopy (GENESYS 10S, Thermo Fisher Scientific, Waltham, MA, USA) was employed to quantify the concentrations of Co and Ni in the leachate. Calibration curves were established using standard solutions and subsequently used to calculate the concentrations of Co and Ni. The absorbance of Co and Ni was measured at wavelengths of 690 nm and 395 nm, respectively. Additionally, ICP-OES analyses were performed to validate the Co and Ni concentrations obtained via UV-vis spectroscopy. To verify whether each chemical component retained its characteristic peaks after DES synthesis and to confirm the formation of DES through hydrogen bonding, Fourier-transform infrared spectroscopy (FTIR; Thermo Fisher Scientific) was conducted. Spectra of the ChCl/PA-based DES, 1.5 M PA, 1 M ChCl, and regenerated ChCl/PA-based DES were collected over the range of 400–4000 cm^{-1}. Changes in valence of Ni and Co during reductive roasting were determined by analysis of X-ray photoelectron spectroscopy (XPS; K-Alpha, Thermo Fisher Scientific, Waltham, MA, USA) using an Al Kα radiation source. The crystalline structures of the cell powder after roasting and the metal precipitates recovered from the solvent extraction process were identified using X-ray diffraction (XRD; ULTIMA 4, Rigaku, Tokyo, Japan) at a scan speed of 2°/min over a 2θ range of 5–90°. The morphology and surface composition of the cell powder were analyzed via scanning electron microscopy (SEM; SU8220, Hitachi High-Technologies, Tokyo, Japan) equipped with energy-dispersive X-ray spectroscopy.

3. Results and discussion

3.1. Metal contents in cell powder

To determine the metal contents in cell powder derived from spent LIBs, both XRF and ICP-OES were employed. Since XRF cannot detect Li, Li concentration was quantified exclusively by ICP-OES. Carbon content was measured using an elemental analyzer (Vario EL, Elementar, Langenselbold, Germany). By integrating data from these analytical techniques, the overall elemental composition of the cell powder was established. Analysis revealed that carbon constitutes the largest fraction, accounting for 41 wt.% of the total composition. Ni was the second most abundant element at 34 wt.%, followed by Mn at 10 wt.%, Co at 8.4 wt.%, and Li at 6.6 wt.%. Based on the elemental composition, it is inferred that various types of nickel-cobalt-manganese (NCM) LIBs were mixed during the dismantling process in recycling.

3.2. Preparation of DESs

To optimize the viscosity and enhance the leaching efficiency of the DES, DIW was added to the DES composed of ChCl and PA at a molar ratio of 1:1, in increments of 5 wt.% ranging from 10 wt.% to 40 wt.%. As shown in Table 1, the optimal leaching efficiency was achieved with the addition of 30 wt.% DIW, resulting in leaching efficiencies of 95.7% and 82.5% for Ni and Co, respectively, under conditions of 120 °C for 2 h and a solid-to-liquid ratio of 15 g/L. Further optimization revealed that a molar ratio of 1:1.5 between ChCl and PA yielded leaching efficiencies of 91.3% for Ni and 100% for Co under the same temperature, duration, solid-to-liquid ratio, and 30 wt.% water content (Table S1).

Table 1. Leaching efficiency of Ni and Co by ChCl-PA DES (1:1 molar ratio) according to DIW content (Leaching conditions: 120 °C for 2 h with 15 g/L of solid-to-liquid ratio)

DIW content (Unit: wt.%)	Leaching efficiency (%)	
	Ni	Co
10	59.6	50.4
15	67.0	51.8
20	78.7	53.1
25	83.4	64.1
30	95.7	82.5
35	91.6	88.5
40	91.5	88.7

Consequently, a DES composition with a molar ratio of 1:1.5 (ChCl:PA) and 30 wt.% DIW was identified as the optimal leaching agent. The structural characteristics and composition of the ChCl-PA DES were evaluated by FTIR analysis (Fig. 1). A distinct -OH stretching band near 2500-3300 cm^{-1} was observed in all samples, indicating the presence of a hydrogen-bonding network essential for DES formation. The spectra further demonstrated that the carboxyl group (-COOH) of PA (C=O, 1700-1725 cm^{-1}) and the hydroxyl group (-OH) of ChCl form hydrogen bonds (2500-3300 cm^{-1}) that maintain the chemical identities of each component (Fig. 1) while imparting unique physicochemical properties to the DES. These findings support that the ChCl-PA DES is formed through complex hydrogen bonding and ion-ion interactions rather than simple physical mixing (Claire et al., 2016). Although previous studies have suggested that the addition of water may disrupt the DES structure (Hammond et al., 2017), the FTIR spectra indicate that the inherent hydrogen-bonding network of the DES remains intact even with the addition of 30 wt.% DIW (Fig. 1). This suggests that water can be used to reduce the viscosity of the DES, thereby facilitating metal leaching.

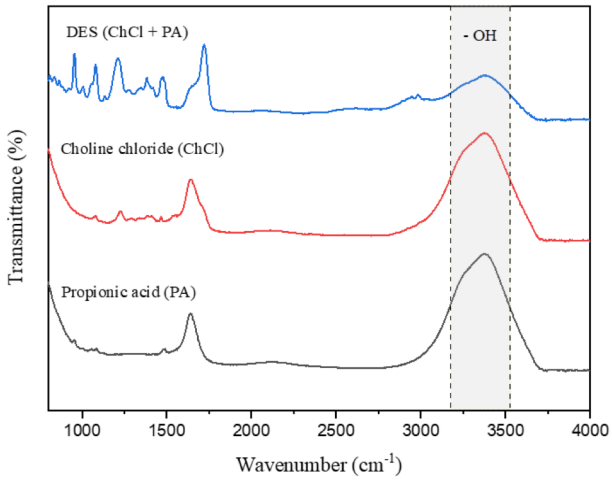

Fig. 1. FTIR spectra of propionic acid (PA), choline chloride (ChCl), and ChCl-PA DES (1:1.5 molar ratio)

3.3. Roasting of cell powder

To determine the optimal conditions for reductive roasting, the leaching efficiency in subsequent DES leaching tests (ChCl:PA molar ratio of 1:1.5, 120 °C, 2 h, 15 g/L solid-to-liquid ratio, and 30 wt.% DIW) was evaluated. As shown in Fig. 2(a), Ni and Co exhibited high leaching efficiencies between 100 °C and 300 °C, achieving complete (100%) leaching at 200 °C. The leaching efficiency of Ni sharply declined at temperatures above 400 °C, leading to the selection of 200 °C as the optimal roasting temperature. Meanwhile, a roasting duration of 2 h was identified as the most effective for maximizing Co and Ni recovery (Fig. 2(b)). Based on these results, roasting at 200 °C for 2 h was established as the optimal condition to maximize Ni and Co recovery during the reductive roasting and subsequent ChCl-PA DES leaching process. To validate the effectiveness of reductive roasting under these conditions, XRD analysis was performed. As the roasting temperature increased, the diffraction peaks corresponding to lithium-nickel-cobalt-manganese-oxide (LNCMO) gradually diminished, while diffraction peaks of metallic Ni and Co appeared at temperatures above 200 °C (Fig. 3). This indicates that LNCMO undergoes dissociation via reduction reactions at the cathode during roasting (Wu et al., 2024). Furthermore, SEM images revealed that the cathode material in the cell powder exhibited less shrinkage and developed surface cracks and open spaces after roasting (Fig. 4). These morphological changes likely facilitate enhanced interaction between the cathode material and leaching agents, thereby improving leaching efficiency. It is reported that reductive transformation of Ni and Co in cathode materials may result in increasing the leaching efficiency of metals in subsequent extraction procedures (Pan and Shen, 2023; Shen and Zhang, 2025). As shown in deconvoluted XPS spectra of cell powder before and after anaerobic roasting (Fig. 5), the anaerobic roasting increased the divalent Ni and Co, supporting that the increase in leaching efficiency after anaerobic roasting may be due to the reductive transformation of Ni (855.4 and 872.9 eV for Ni^{2+} $2p_{3/2}$ and $2p_{1/2}$, respectively) and Co (781.35 and 796.65 eV for Co^{2+} $2p_{3/2}$ and $2p_{1/2}$, respectively). In contrast, the effect of roasting temperature on the leaching of Ni and Co under the given conditions was not clear. Though a slight difference in leaching efficiency between 200 and 500 °C of roasting temperature was observed, the reductive transformation of Ni and Co was not much changed. It appears that increasing the roasting temperature may not significantly enhance the reductive transformation of Ni and Co under the given conditions. In addition to carbothermal reduction of cell powder, it is likely that other possible reduction mechanisms may be involved in the anaerobic roasting at 200 °C, which remains to be further studied.

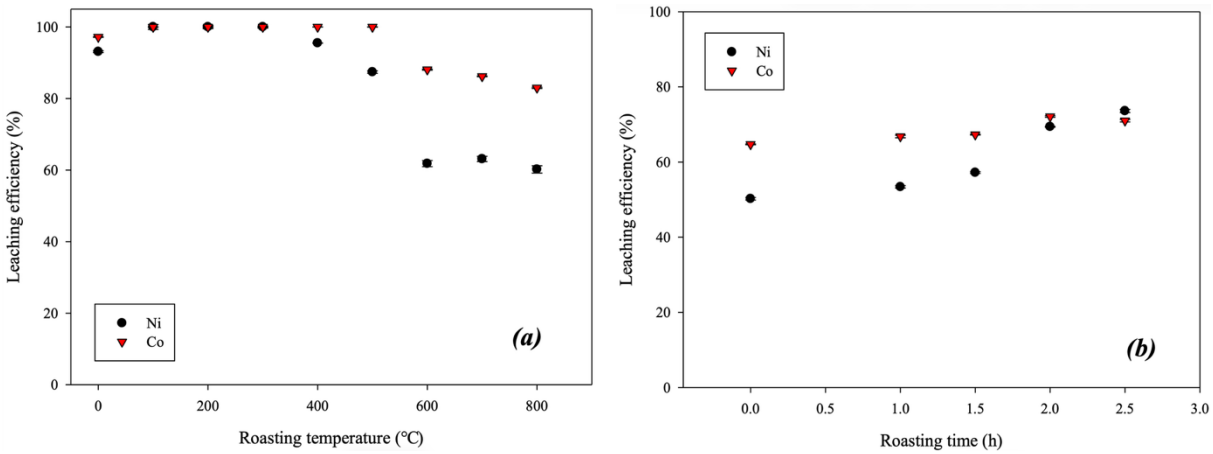

Fig. 2. Leaching efficiency of nickel and cobalt by ChCl-PA DES (1:1.5 molar ratio and 30 wt.% DIW) after reductive roasting according to (a) roasting temperature (roasting time: 2 h) and (b) roasting time (roasting temperature: 500 °C). (Leaching conditions: 120 °C for 2 h with a 15 g/L solid-to-liquid ratio) Data points are averages of triplicate samples, and error bars represent one standard deviation

3.4. Leaching of cell powder with ChCl-PA DES

After reductive roasting at 200 °C for 2 h, the optimal leaching conditions were determined by varying the leaching temperature, leaching time, and solid-to-liquid ratio. Starting with a leaching time of 120 min and a solid-to-liquid ratio of 15 g/L, the leaching efficiency for Co and Ni was maximized at temps.

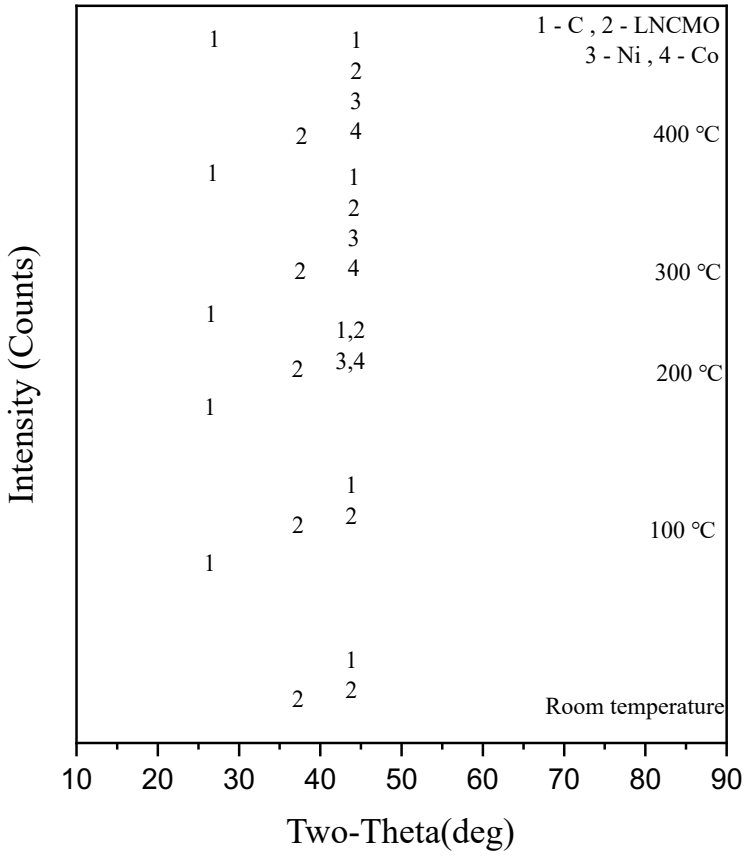

Fig. 3. XRD patterns of cell powder roasted at various temperatures for 2 h. The peaks numbered 1, 2, 3, and 4 represent carbon (C), lithium-nickel-cobalt-manganese oxide (LNCMO), nickel (Ni), and cobalt (Co), respectively

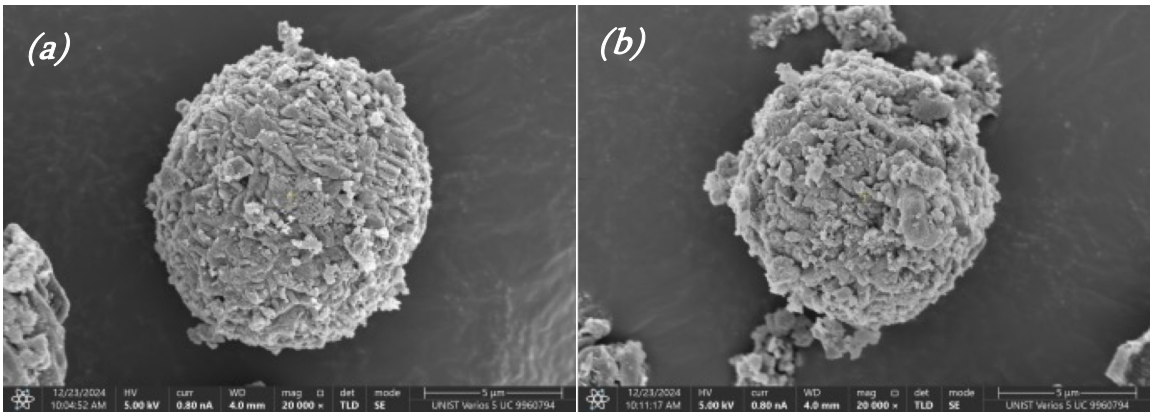

Fig. 4. SEM images of cell powder (a) before and (b) after roasting at 200℃

above 80 °C (Fig. 6(a)), setting the optimal temperature at 80 °C. Subsequently, with the temperature fixed at 80 °C and a solid-to-liquid ratio of 15 g/L, a leaching time of 120 min ensured maximum leaching efficiency for both metals (Fig. 6(b)). Finally, at 80 °C and 120 min, the optimal solid-to-liquid ratio was identified as 15 g/L (Fig. 6(c)). These results confirmed that complete leaching of Co and Ni from the cell powder could be achieved under the conditions of 80 °C, 120 min, and 15 g/L. The high extraction efficiencies of Ni, Co, Mn, and Li from cell powder in the ChCl–PA DES system can be attributed to a complex interplay between chemical leaching and coordination chemistry (Alhashim, 2023). The primary dissolution mechanism likely begins with proton-promoted attack on the metal oxide lattice. As a strong hydrogen bond donor, PA supplies a high concentration of protons (H^+), which protonate oxide ions in the metal oxides to form water. This destabilizes the solid matrix and facilitates

the release of metal cations into the solvent (Pateli, 2020). At the same time, propionate may act as a ligand, forming metal–ligand complexes in the liquid phase. ChCl also plays a critical role by providing a concentrated source of chloride ions (Cl^-), which promote metal dissolution through complexation (Pateli, 2020). Once liberated from the oxide lattice, metal ions can coordinate with chloride ions to form stable chloro-complexes, such as $NiCl_4^{2-}$ and $CoCl_4^{2-}$. This metal speciation helps prevent reprecipitation of the dissolved metals. By sequestering metal ions into stable anionic complexes, the DES maintains a high solubilizing capacity.

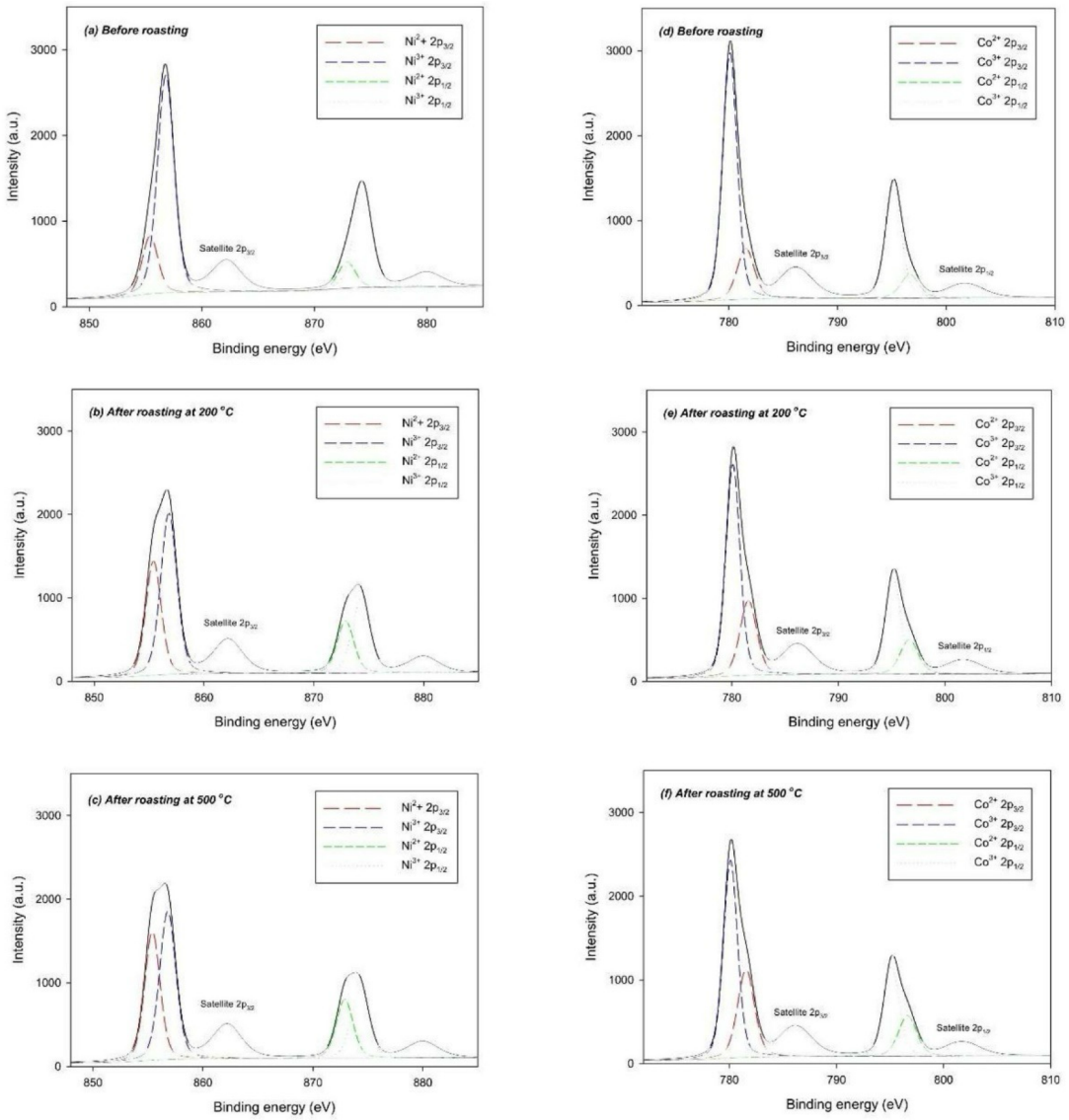

Fig. 5. Deconvoluted XPS spectra of cell powder [Ni2p: (a) before roasting, (b) after roasting at 200 °C, and (c) after roasting at 500 °C; Co2p: (d) before roasting, (e) after roasting at 200 °C, and (f) after roasting at 500 °C]

To reduce the leaching time, NTA was added due to its ability to form strong complexes with metal ions, thereby increasing their solubility and facilitating faster transport into the solution (Wang et al., 2022). As shown in Fig. 7(a), the addition of 0.07 M NTA enabled complete leaching of Co and Ni without prior reductive roasting, demonstrating that NTA significantly enhances the dissolution of these metals and that 0.07 M is sufficient for complex formation under the tested conditions. Subsequent experiments involved reducing the leaching time in 10-min intervals from 120 to 50 min after roasting at 80 °C and 15 g/L with 0.07 M NTA. Complete recovery of Co and Ni was achieved at 80 °C for 60 min with 0.07 M NTA (Fig. 7(b)). This indicates that 0.07 M NTA provides an adequate concentration of chelating agents necessary for metal ion binding without causing excessive solvent viscosity or compromising complex stability, which can occur at higher NTA concentrations. ICP-OES analysis

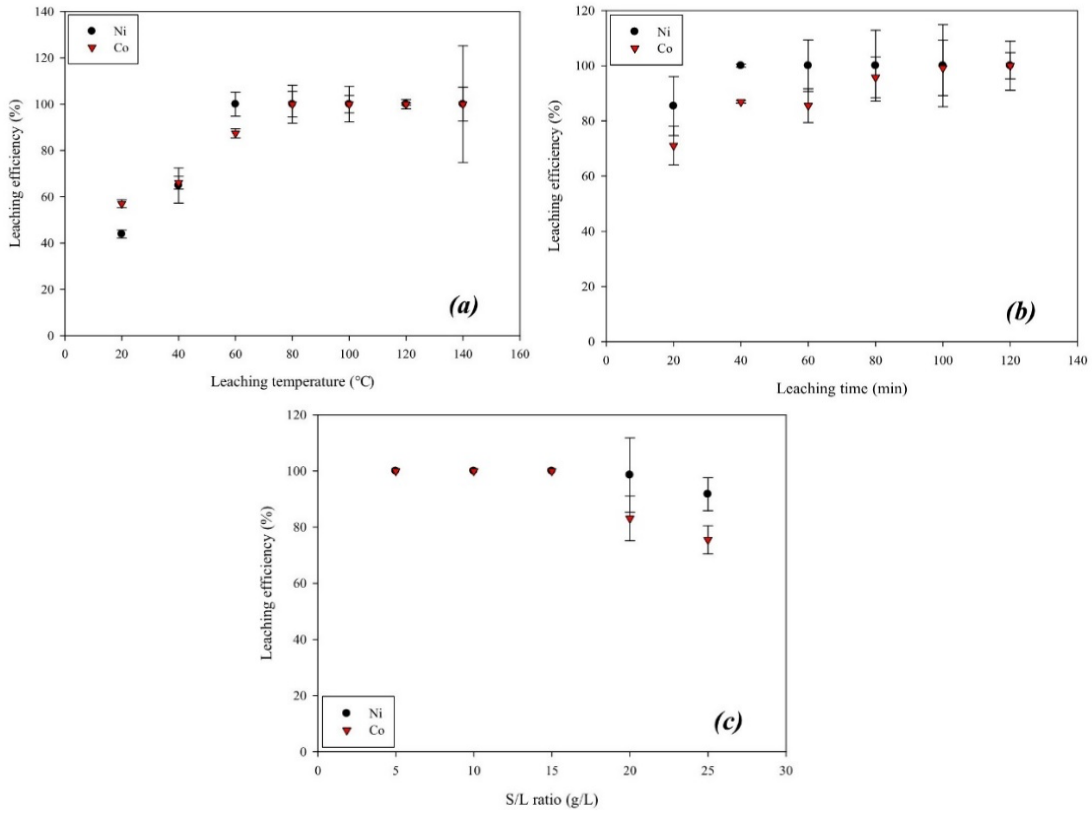

Fig. 6. Leaching efficiency of nickel and cobalt by ChCl-PA DES after reductive roasting (200 °C for 2 h) according to (a) leaching temperature (leaching time: 120 min, solid-liquid ratio: 15 g/L), (b) leaching time (leaching temperature: 80 °C, solid-liquid ratio: 15 g/L), and (c) solid-to-liquid ratio (leaching temperature: 80 °C, leaching time: 120 min). The molar ratio of ChCl-to-PA is 1:1.5, and DIW content is 30 wt.%. Data points are averages of triplicate samples, and error bars represent one standard deviation

further confirmed the complete leaching efficiencies of Co and Ni (Fig. S2). Based on the mass balance between the initial metal contents in the cell powder and the concentrations measured in the leachate, leaching efficiencies for Li and Mn were calculated as 98.5% and 100%, respectively (Fig. S2), providing direct evidence supporting the optimal leaching conditions of 80 °C, 60 min, and 15 g/L. Shorter leaching times (40 and 50 min) resulted in a significant decrease in leaching efficiencies for all metals (Fig. S2).

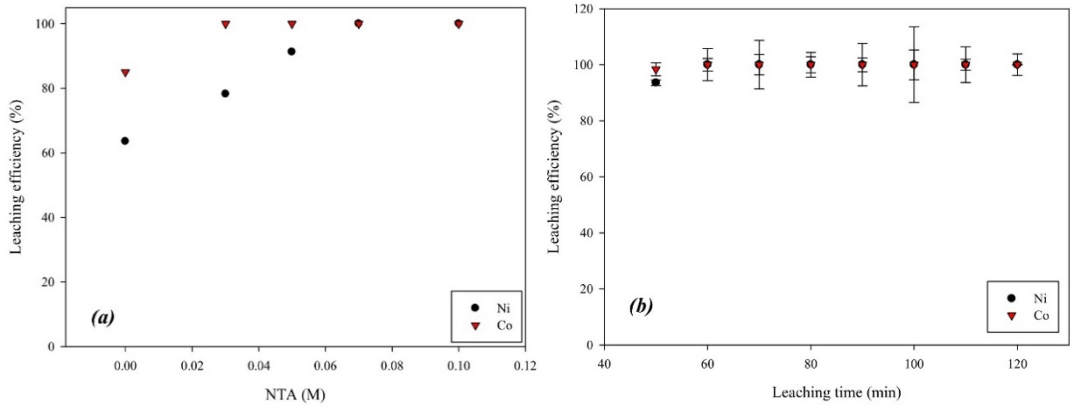

Fig. 7. Leaching efficiency of nickel and cobalt by ChCl-PA DES with NTA according to (a) NTA concentration (leaching time: 120 min, no roasting) and (b) leaching time (NTA concentration: 0.07 M after roasting at 200 °C for 2 h). Leaching temperature, solid-to-liquid ratio, molar ratio of ChCl-to-PA, and DIW content are 80 °C, 15 g/L, 1:1.5, and 30 wt.%, respectively. Data points are averages of triplicate samples, and error bars represent one standard deviation

3.5. Solvent extraction of metals from leachate

In the initial stage of solvent extraction, Mn was selectively extracted using 0.6 M D2EHPA, followed by stripping with 1 M sulfuric acid and pH adjustment to recover Mn as manganese hydroxide (Fig. 8(a)). The XRD pattern of the precipitate confirmed the formation of manganese hydroxide (Anandan et al., 2013) and demonstrated that Mn can be selectively separated via strong interactions with 0.6 M D2EHPA (Nadimi et al., 2021). In the second stage, Co was recovered using 20 vol.% Cyphos IL 104, stripped with 1 M sulfuric acid, and precipitated as cobalt hydroxide by adjusting the pH above 7, as confirmed by XRD analysis (Fig. 8(b)) (Si et al., 2018). This process is facilitated by Cyphos IL 104's high affinity for Co ions, enabling effective separation (Yuda et al., 2024). Subsequently, Ni was recovered by precipitation as nickel oxalate through the addition of oxalic acid. The presence of nickel oxalate was confirmed by XRD analysis (Fig. 8(c)), consistent with previous studies (Kim et al., 2019). In the final stage, Li remaining in the aqueous phase was recovered as lithium oxalate by evaporating the solution, supported by the XRD pattern shown in Fig. 8(d) (Chen et al., 2015; Tian et al., 2022). These results indicate that each metal ion can be selectively separated and recovered as metal precipitates under specific chemical conditions. In order to confirm the purity of each metal at each extraction stage, each precipitate was dried and dissolved by aqua regia, and elemental compositions of Mn, Co, Ni, and Li in the precipitate at each solvent extraction stage were determined by ICP-OES. The results confirmed that the obtained precipitates at solvent extraction stages did not include other elements higher than 0.01 mg/kg. It should be noted that the determination of elements in ICP-OES analysis only included Li, Ni, Co, and Mn. Therefore, it cannot be completely ruled out that other elements may be included as impurities in each precipitate, which may need to be further investigated.

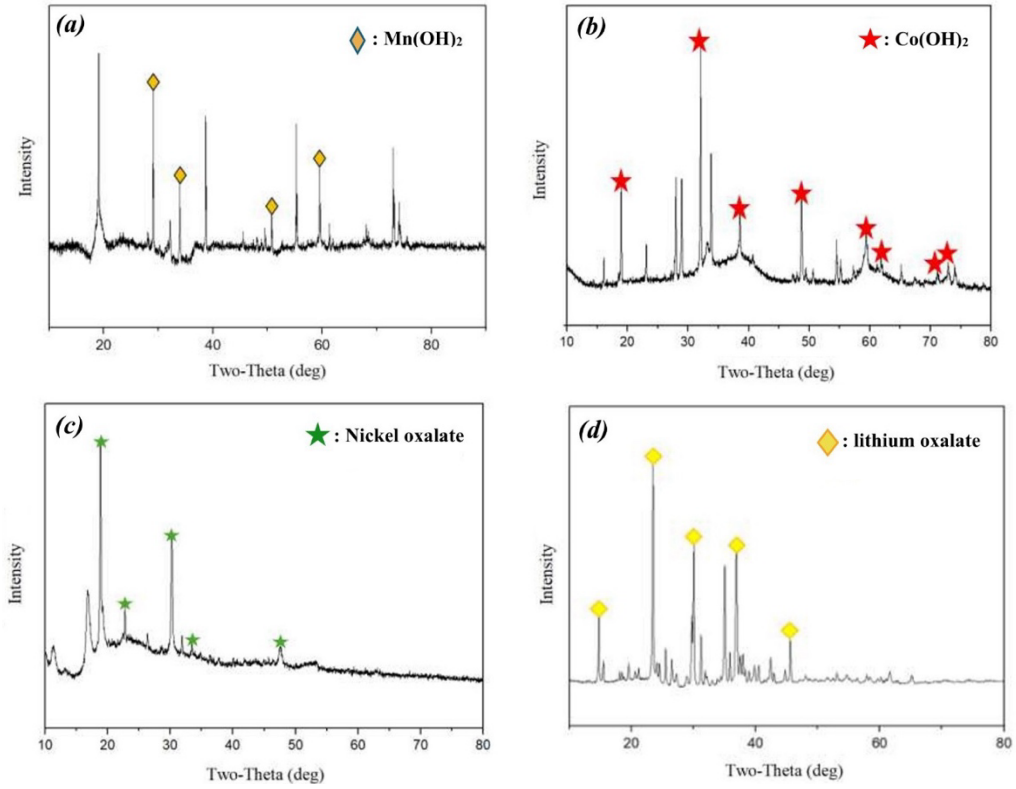

Fig. 8. XRD patterns of (a) manganese, (b) cobalt, (c) nickel, and (d) lithium precipitates collected from a stepwise solvent extraction procedure. Two-theta values of manganese hydroxide, cobalt hydroxides, nickel oxalate, and lithium oxalate are denoted according to XRD data obtained by Anandan et al. (2013), Si et al. (2018), Kim et al. (2019), and Tian et al. (2022), respectively.

3.6. Reusability of ChCl-PA DES

In this study, DES was effectively employed to leach Co, Ni, Mn, and Li from cell powder. To evaluate the reusability of DES after solvent extraction for metal recovery, leaching experiments using recovered

DES were conducted. UV-vis spectroscopy analysis of the DES leachate (Fig. S3) showed absorption peaks for Ni and Co at 395 nm and 690 nm, respectively, before solvent extraction, which disappeared after extraction, indicating the complete removal of these metals from DES during the solvent extraction process. FTIR spectra of the pristine and reused DES exhibited identical vibration bands at the same wavelengths (Figs. S4(a) and S4(b)), demonstrating that the main components of the DES—formed via hydrogen bonding between ChCl and PA—maintain their original chemical characteristics after the roasting-leaching-extraction cycle. This chemical stability suggests that ChCl-PA DES can be reused without additional physical or chemical treatment. However, leaching with reused DES resulted in decreased leaching efficiencies even under the optimal conditions of 80 °C, 60 min, and 15 g/L (Fig. S4). Upon first reuse, leaching efficiencies for Ni and Co decreased to 86.2% and 89.1%, respectively, representing reductions of 13.8% and 10.1% compared to pristine DES. The second reuse further decreased efficiencies to 60.9% and 62.4% for Ni and Co, respectively, and from the third reuse onward, efficiencies dropped below 50% for both metals (Fig. S4). These declines in performance, despite the chemical structure of DES remaining intact as confirmed by FTIR, are likely attributable to factors such as increased viscosity from water evaporation, loss of DES components due to solvent evaporation, and dilution during solvent extraction over multiple reuse cycles. This highlights the necessity of strategies to minimize evaporation and maintain the optimal DES concentration during metal recovery. Further research is needed to develop methods for adjusting operating parameters to maintain the leaching capacity of DES or introducing additives to stabilize the solution without compromising its chemical stability.

4. Conclusions

This study presents an efficient and sustainable recycling procedure for the recovery of valuable metals from cell powder in spent LIBs by integrating reductive roasting, leaching with DES and NTA, and solvent extraction. Reductive roasting at 200 °C for 2 h effectively loosened the cathode materials, enhancing subsequent leaching performance. The DES, composed of ChCl and PA at a 1:1.5 molar ratio with 30 wt.% DIW, achieved complete leaching efficiencies for Ni, Co, and Mn, and 98.5% for Li at 80 °C for 60 min in the presence of 0.07 M NTA. Although the DES exhibited reusability, a noticeable decline in leaching efficiency (10–20%) was observed with each reuse cycle, likely due to dilution and evaporation of DES components during the recycling process. The proposed process offers an environmentally friendly and sustainable alternative for hydrometallurgical battery recycling, contributing to resource circulation, reducing dependence on raw materials, and minimizing environmental impact. Further studies on practical applications and economic evaluations are required for future development.

Acknowledgments

This work was supported by the Korea Institute for Advancement of Technology (KIAT) grant funded by the Korea Government (MOTIE) (P0020614, HRD Program for Industrial Innovation). This work was also in part supported by the Regional Innovation Cluster Development (R&D) by the Ministry of Trade, Industry, and Energy (MOTIE, South Korea) [Project Name: Open Innovation Project for Convergence Industry of Battery/Fuel Cell for Mobility Electrification and Energy Production/Storage (P0025406)].

References

ALHASHIM, S.H., BHATTACHARYYA, S., TROMER, R., KABBANI, A., BABU, G., OLIVEIRA, E.F., GALVAO, D.S., AJAYAN, P.M., 2023. *Mechanistic study of lithium-ion battery cathode recycling using deep eutectic solvents*. ACS Sustainable Chem. Eng. 11, 6914–6922. https://pubs.acs.org/doi/10.1021/acssuschemeng.2c06571

ANANDAN, S., ARIVANANDHAN, M., SONAWANE, S.H., ASHOKKUMAR, M., 2013. *Sonochemical synthesis of manganese (II) hydroxide for supercapacitor applications.* Mater. Res. Bull. 48, 3357–3364. https://doi.org/10.1016/j.materresbull.2013.05.021

BRITISH GEOLOGICAL SURVEY (BGS), 2018. Battery raw materials: Briefing note on raw materials for batteries in electric vehicles, Nottingham.

CHEN, L., ZHANG, J., WANG, Z., 2021. *Engineering a tandem leaching system for the highly selective recycling of valuable metals from spent Li-ion batteries.* Green Chem. 23, 2177–2184. https://doi.org/10.1039/D0GC03820B

CHEN, X., ZHAO, Y., ZHOU, T., 2015. *Separation and recovery of metal values from leaching liquor of mixed-type of spent lithium-ion batteries*. Sep. Purif. Technol. 144, 197–205. https://doi.org/10.1016/j.seppur.2015.02.006

CLAIRE, D., SIMONA, C., FRANÇOIS, J., ISABELLE, G., 2016. *Doubly ionic hydrogen bond interactions within the choline chloride–urea deep eutectic solvent*. Phys. Chem. Chem. Phys. 18, 18145–18160. https://doi.org/10.1039/C6CP02815B

DALINI, N., RASHCHI, F., MOSTOUFI, N., SABA, M., 2020. *A review on environmental, economic and hydrometallurgical processes of recycling spent lithium-ion batteries*. Miner. Process. Extr. Metall. Rev. 42, 451–472. https://doi.org/10.1080/08827508.2020.1781628

EGBUE, O., LONG, S., 2012. *Critical issues in the supply chain of lithium for electric vehicle batteries*. Eng. Manag. J. 24, 52–62. https://doi.org/10.1080/10429247.2012.11431947

HAMMOND, O.S., BOWRON, D.T., EDLER, K.J., 2017. *The effect of water upon deep eutectic solvent nanostructure: an unusual transition from ionic mixture to aqueous solution*. Angew. Chem. 129, 9914–9917. https://doi.org/10.1002/anie.201702486

HUA, Y., XIONG, P., MA, X., ZHANG, W., ZHAO, X., 2022. *Ionization potential-based design of deep eutectic solvent for recycling of spent lithium-ion batteries*. Chem. Eng. J. 436, 133200. https://doi.org/10.1016/j.cej.2021.133200

INTERNATIONAL ENERGY AGENCY, 2024. Global EV Outlook 2024, Paris.

JI, Y., YANG, F., WANG, Y., 2021. *Direct recycling technologies of cathode in spent lithium-ion batteries*. Clean Technol. Recycl. 1, 124–151.

KIM, Y.-C., LEE, J.-H., SEO, H.-J., 2019. *Recovery of rare metals from the waste secondary lithium-ion battery cathode active materials using lactic acid and oxalic acid*. J. Korean Chem. Soc. 63, 446–452.

KISTI DATA ANALYSIS DEPARTMENT, 2021. Business opportunities and promotion strategies for companies in line with the expansion of the electric vehicle battery recycling and reuse industry (ASTI MARKET INSIGHT; 2021-004), Daejeon.

KUDŁAK, B., OWCZAREK, K., NAMIEŚNIK, J., 2015. *Selected issues related to the toxicity of ionic liquids and deep eutectic solvents – a review*. Environ. Sci. Pollut. Res. 22, 11975–11992. https://doi.org/10.1007/s11356-015-4794-y

LI, L., LIU, J., SHI, X., WANG, D., 2013. *Recovery of metals from spent lithium-ion batteries with organic acids as leaching reagents and environmental assessment*. J. Power Sources 233, 180–189. https://doi.org/10.1016/j.jpowsour.2012.12.089

LI, Y., CHANG, Z., XIE, T., LI, L., ZHANG, X., LI, J., 2021. *Separation of valuable metals from mixed cathode materials of spent lithium-ion batteries by single-stage extraction*. Korean J. Chem. Eng. 38, 2113–2121. https://doi.org/10.1007/s11814-021-0834-0

LIU, C., ZHENG, F., YANG, Z., 2019. *Recycling of spent lithium-ion batteries in view of lithium recovery: a critical review*. J. Clean. Prod. 228, 801–813. https://doi.org/10.1016/j.jclepro.2019.04.304

LIU, Y., WANG, C., ZHANG, M., 2023. *Revolutionizing the automotive industry: Tesla's innovative marketing strategies in the face of changes*. Highlights Bus. Econ. Manag. 23, 312–318.

LUO, Y., DENG, Y., SHI, H., YANG, H., YIN, C., OU, L., 2024. *Green and efficient recycling method for spent Ni–Co–Mn lithium batteries utilizing multifunctional deep eutectic solvents*. J. Environ. Manage. 351, 119814. https://doi.org/10.1016/j.jenvman.2023.119814

LUO, Y., YIN, C., OU, L., 2023. *A green and efficient combination process for recycling spent lithium-ion batteries*. J. Clean. Prod. 396, 136552. https://doi.org/10.1016/j.jclepro.2023.136552

MAKUZA, B., TIAN, Q., GUO, X., LIU, Y., XU, Z., 2021. *Pyrometallurgical options for recycling spent lithium-ion batteries: a comprehensive review*. J. Power Sources 491, 229622. https://doi.org/10.1016/j.jpowsour.2021.229622

MESHRAM, P., MISHRA, A., SAHU, R., 2020. *Environmental impact of spent lithium-ion batteries and green recycling perspectives by organic acids – a review*. Chemosphere 242, 125291. https://doi.org/10.1016/j.chemosphere.2019.125291

MISHRA, B.B., DEVI, N., SARANGI, K., 2020. *Recovery of samarium and cobalt from Sm–Co magnet waste using a phosphonium ionic liquid Cyphos IL 104*. J. Sustain. Metall. 6, 410–418. https://doi.org/10.1007/s40831-020-00283-6

MIZUSHIMA, K., JONES, P.C., WISEMAN, P.J., GOODENOUGH, J.B., 1980. *Li_xCoO_2 ($0 < x \leq 1$): a new cathode material for batteries of high energy density*. Mater. Res. Bull. 15, 783–789. https://doi.org/10.1016/0025-5408(80)90012-4

MROZIK, W., RAJAEIFAR, M.A., HEIDRICH, O., 2021. *Environmental impacts, pollution sources and pathways of spent lithium-ion batteries*. Energy Environ. Sci. 14, 6099–6121. https://doi.org/10.1039/D1EE00691F

NADIMI, H., JALALIAN KARAZMOUDEH, N., 2021. *Selective separation and purification of Mn from Co and Ni in waste mobile phone lithium-ion batteries using D2EHPA via solvent extraction method*. J. Sustain. Metall. 7, 653–665. https://doi.org/10.1007/s40831-021-00371-1

OLIVETTI, E.A., CEDER, G., GAUSTAD, G.G., FU, X., 2017. *Lithium-ion battery supply chain considerations: analysis of potential bottlenecks in critical metals*. Joule 1, 229–243. https://doi.org/10.1016/j.joule.2017.08.019

PAN, C., SHEN, Y., 2023. *Pyrometallurgical recycling of spent lithium-ion batteries from conventional roasting to synergistic pyrolysis with organic wastes*. J. Energy Chem. 85, 547–561. https://doi.org/10.1016/j.jechem.2023.06.040

PADWAL, C., NATARAJAN, S.S., MHASKE, S., 2022. *Deep eutectic solvents: green approach for cathode recycling of Li-ion batteries*. Adv. Energy Sustain. Res. 3, 2100133. https://doi.org/10.1002/aesr.202100133

PATELI, I.M., BINNEMANS, K., RIAÑO, S., 2020. *The effect of pH and hydrogen bond donor on the dissolution of metal oxides in deep eutectic solvents*. Green Chem. 22:5476–5486. https://doi.org/10.1039/D0GC02023K

PETERS, J.F., BAUMANN, M., ZIMMERMANN, B., 2017. *The environmental impact of Li-ion batteries and the role of key parameters – a review*. Renew. Sustain. Energy Rev. 67, 491–506. https://doi.org/10.1016/j.rser.2016.08.039

QIAO, W., ZHANG, R., WEN, Y., WANG, X., WANG, Z., TANG, G., LIU, M., KANG, H., SAI, Z., HWANG, J.Y., LIU, C., 2024. *Green solvents in battery recycle: status and challenges*. J. Mater. Chem. A 12, 11235–11265. https://doi.org/10.1039/D3TA07905H

RADOŠEVIĆ, K., CVJETKO, I., KOPJAR, N., 2015. *Evaluation of toxicity and biodegradability of choline chloride-based deep eutectic solvents*. Ecotoxicol. Environ. Saf. 112, 46–53. https://doi.org/10.1016/j.ecoenv.2014.09.034

RADOŠEVIĆ, K., KOVAČEVIĆ, G., JURINIĆ, I., 2016. *Comparative in vitro study of cholinium-based ionic liquids and deep eutectic solvents toward fish cell line*. Ecotoxicol. Environ. Saf. 131, 30–36. https://doi.org/10.1016/j.ecoenv.2016.05.005

REINHART, L., VRUCAK, D., WOESTE, R., LUCAS, H., ROMBACH, E., FRIEDRICH, B., LETMATHE, P., 2023. *Pyrometallurgical recycling of different lithium-ion battery cell systems: economic and technical analysis*. J. Clean. Prod. 416, 137834. https://doi.org/10.1016/j.jclepro.2023.137834

RYBKA, P., REGEL-ROSOCKA, M., 2012. *Nickel (II) and cobalt (II) extraction from chloride solutions with quaternary phosphonium salts*. Sep. Sci. Technol. 47, 1296–1302. https://doi.org/10.1080/01496395.2012.672532

SCHIAVI, P.G., CARERI, M., BIANUCCI, R., 2021. *Selective recovery of cobalt from mixed lithium-ion battery wastes using deep eutectic solvent*. Chem. Eng. J. 417, 129249. https://doi.org/10.1016/j.cej.2021.129249

SHEN, Y., ZHANG, S., 2025. *Recent advances in sustainable reductive roasting for spent lithium-ion batteries recycling*. Energy Storage Mater. 79, 104358. https://doi.org/10.1016/j.ensm.2025.104358

SI, Y., LIU, Z., ZHANG, H., WANG, J., SUN, X., 2018. *An ultrasonication-assisted cobalt hydroxide composite with enhanced electrocatalytic activity toward oxygen evolution reaction*. Materials 11, 1912. https://doi.org/10.3390/ma11101912

SMITH, E.L., ABBOTT, A.P., RYDER, K.S., 2014. *Deep eutectic solvents (DESs) and their applications*. Chem. Rev. 114, 11060–11082. https://doi.org/10.1021/cr300162p

TIAN, Y., LI, X., HOU, J., ZHANG, M., ZHANG, R., 2022. *A weak acidic and strong coordinated deep eutectic solvent for recycling of cathode from spent lithium-ion batteries*. ChemSusChem 15, e202200524. https://doi.org/10.1002/cssc.202200524

TRADING ECONOMICS, 2023. Nickel. https://ko.tradingeconomics.com/commodity/nickel.

TRAN, M.K., LIN, Z., WANG, Y., 2019. *Deep eutectic solvents for cathode recycling of Li-ion batteries*. Nat. Energy 4, 339–345. https://doi.org/10.1038/s41560-019-0368-4

VIECELI, N., MARTINS, M.A., ESPINOSA, D.C.S., TENÓRIO, J.A.S., 2023. *Recycling of Li-ion batteries from industrial processing: upscaled hydrometallurgical treatment and recovery of high purity manganese by solvent extraction*. Solvent Extr. Ion Exch. 41, 205–220. https://doi.org/10.1080/07366299.2023.2165405

WANG, S., LIU, F., WANG, Q., 2022. *Recycling of zinc oxide dust using ChCl-urea deep eutectic solvent with nitrilotriacetic acid as complexing agents*. Miner. Eng. 175, 107295. https://doi.org/10.1016/j.mineng.2021.107295

WANG, Z., ZHANG, H., LI, Z., 2022. *Deep eutectic solvents (DESs) for green recycling of wasted lithium-ion batteries (LIBs): progress on pushing the overall efficiency*. Min. Metall. Explor. 39, 2149–2165. https://doi.org/10.1007/s42461-022-00660-7

WELLENS, S., THIJS, B., BINNEMANS, K., 2013. *Separation of cobalt and nickel by solvent extraction with two mutually immiscible ionic liquids*. Phys. Chem. Chem. Phys. 15, 9663–9669. https://doi.org/10.1039/c3cp50819f

WHITTINGHAM, M.S., 1976. *Electrical energy storage and intercalation chemistry*. Science 192, 1126–1127. https://doi.org/10.1126/science.192.4244.1126

WU, X., LI, C., ZHANG, Y., 2024. *Influence mechanism of phase change on leaching of metal elements from ternary lithium-ion battery waste in citric acid*. JOM 76, 1576–1586. https://doi.org/10.1007/s11837-023-06083-z

XU, P., DAI, Q., GAO, H., LIU, H., ZHANG, M., LI, M., CHEN, Y., AN, K., MENG, Y.S., LIU, P., LI, Y., SPANGENBERGER, J.S., GAINES, L., LU, J., CHEN, Z., 2020. *Efficient direct recycling of lithium-ion battery cathodes by targeted healing*. Joule 4, 2609–2626. https://doi.org/10.1016/j.joule.2020.10.008

YAN, Z., SATTAR, A., LI, Z., 2023. *Priority lithium recovery from spent Li-ion batteries via carbothermal reduction with water leaching*. Resour. Conserv. Recycl. 192, 106937. https://doi.org/10.1016/j.resconrec.2023.106937

YAO, Y., WANG, Q., ZHANG, X., 2018. *Hydrometallurgical processes for recycling spent lithium-ion batteries: a critical review*. ACS Sustain. Chem. Eng. 6, 13611–13627. https://doi.org/10.1021/acssuschemeng.8b03545

YUDA, A.P.T., WIDODO, W., HIDAYAT, T.W., HIDAYATI, N., 2024. *Separation of nickel and cobalt from nitrate leaching solutions of laterite ore by solvent extraction using trihexyltetradecylphosphonium bis(2,4,4-trimethyl pentyl) phosphinate*. E3S Web Conf. 503. https://doi.org/10.1051/e3sconf/202450306007

ZADEH, M.A.H., CUNNINGHAM, S., GRAY, D., AZIMI, G., 2026. *Selective lithium pre-leaching from spent NMC black mass via pyrolysis and controlled leaching*. Waste Manage. 212, 115339. https://doi.org/10.1016/j.wasman.2026.115339

Supplementary Material

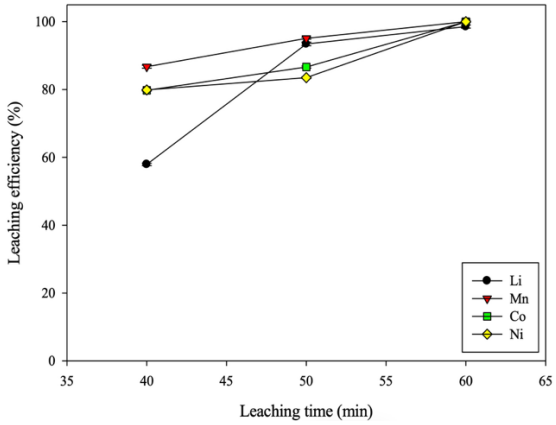

Fig. S1. Leaching efficiency of nickel, cobalt, lithium, and manganese by ChCl-PA DES with NTA (0.07 M) after reductive roasting (200 °C for 2 h). (Leaching temperature: 80 °C, leaching time: 60 min, solid-liquid ratio: 15 g/L). Concentrations of nickel, cobalt, lithium, and manganese were determined using ICP-OES. Molar ratio of ChCl-to-PA is 1:1.5, and DIW content is 30 wt.%. Data points are the average of triplicate samples, and error bars represent one standard deviation

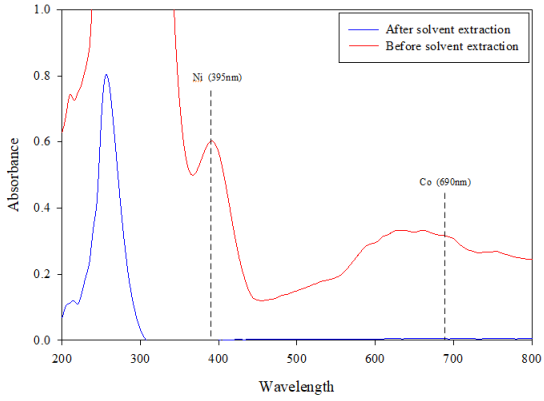

Fig. S2. UV-vis spectra of the leachate from leaching with ChCl-PA DES (1:1.5 molar ratio) before and after solvent extraction

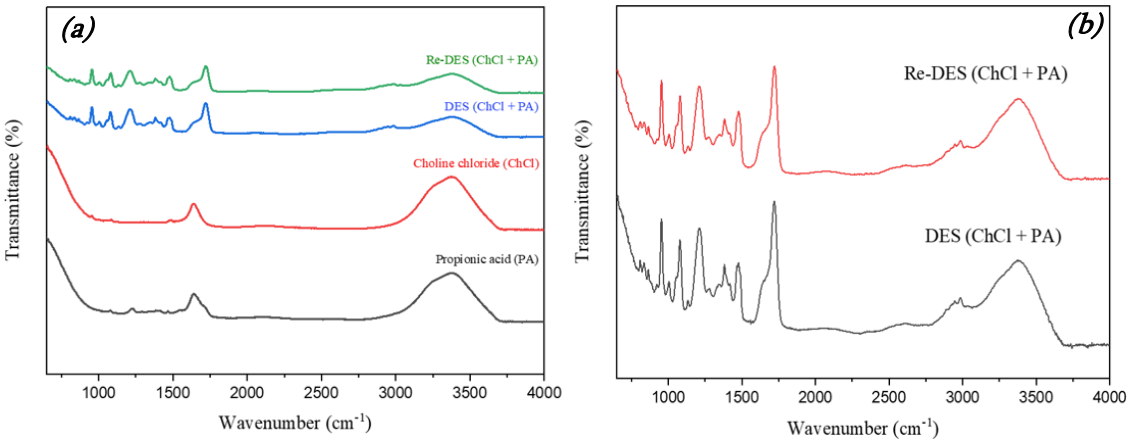

Fig. S3. FTIR (a) spectra of reused DES (Re-DES, ChCl-PA), DES (ChCl-PA), ChCl, and PA, and (b) magnified spectra of Re-DES (ChCl-PA) and DES (ChCl-PA). The molar ratio of ChCl-to-PA is 1:1.5, and DIW content is 30 wt.%. (Leaching temperature: 80℃, leaching time: 60 min, solid-liquid ratio: 15 g/L, and NTA concentration: 0.07 M)

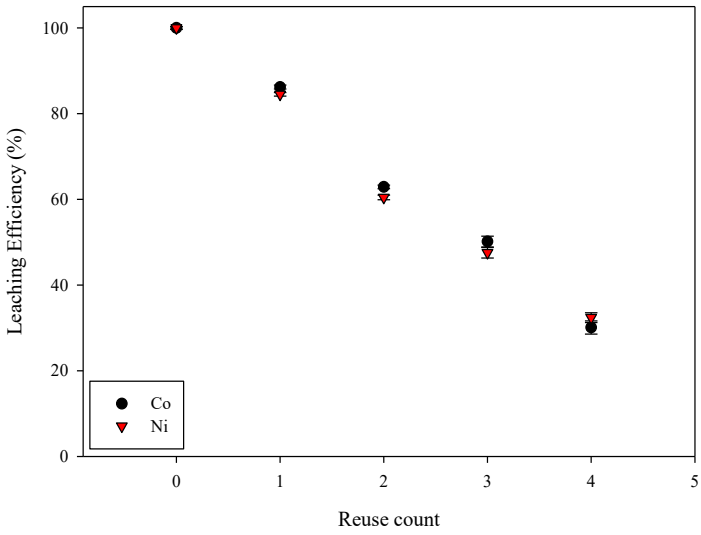

Fig. S4. Leaching efficiency of nickel and cobalt with reused ChCl-PA DES. Molar ratio of ChCl-to-PA is 1:1.5, and DIW content is 30 wt.%. (Leaching temperature: 80℃, leaching time: 60 min, solid-liquid ratio: 15 g/L, and NTA concentration: 0.07 M)